Environmental Science & Technology

pubs.acs.org/est

Article

# Policy-Related Gains in Urban Air Quality May Be Offset by Increased Emissions in a Warming Climate

Cong Cao, Drew R. Gentner,* Róisín Commane, Ricardo Toledo-Crow, Luke D. Schiferl, and John E. Mak*

Cite This: *Environ. Sci. Technol.* 2023, 57, 9683−9692

Read Online

ACCESS | Metrics & More | Article Recommendations | Supporting Information



**ABSTRACT:** Air quality policies have made substantial gains by reducing pollutant emissions from the transportation sector. In March 2020, New York City's activities were severely curtailed in response to the COVID-19 pandemic, resulting in 60−90% reductions in human activity. We continuously measured major volatile organic compounds (VOCs) during January−April 2020 and 2021 in Manhattan. Concentrations of many VOCs decreased significantly during the shutdown with variations in daily patterns reflective of human activity perturbations, resulting in a temporary ∼28% reduction in chemical reactivity. However, the limited effect of these dramatic measures was outweighed by larger increases in VOC-related reactivity during the anomalously warm spring 2021. This emphasizes the diminishing returns from transportation-focused policies alone and the risk of increased temperature-dependent emissions undermining policy-related gains in a warming climate.

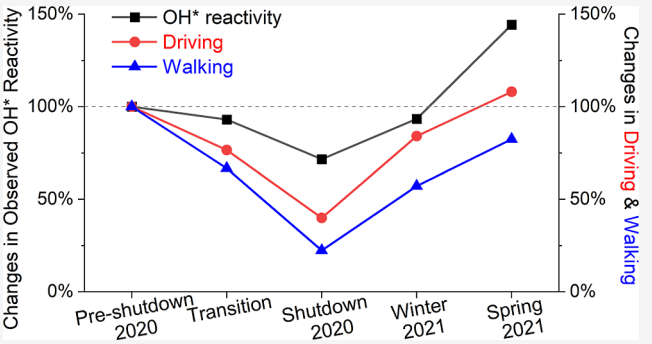


**KEYWORDS:** *urban air quality, volatile organic compound (VOC) emissions, air pollution policy, mobile sources, volatile chemical products (VCPs)*

## 1. INTRODUCTION

Volatile organic compounds (VOCs) play a central role in atmospheric chemistry and urban air quality as reactive precursors to the formation of tropospheric ozone and secondary organic aerosol (SOA), a major component of airborne particulate matter (e.g., $PM_{2.5}$).[1,2] VOCs are emitted from a diverse, but uncertain, mix of biogenic and anthropogenic sources and can negatively impact human health through both direct exposure and formation of secondary air pollution (i.e., ozone, SOA).[3−5] With successful reductions in anthropogenic VOC emissions from motor vehicles and other major combustion-related sources across the U.S., a broader range of understudied, distributed sources [e.g., volatile chemical products (VCPs)] are now responsible for the majority of reactive VOC emissions to urban areas.[6−9] This underconstrained mix of anthropogenic VOC sources includes emissions from chemical products and materials, such as paints, solvents, adhesives, cleaning agents, and personal care products, as well as cooking and distributed fuel combustion.[6,7,10,11]

The successful refinement of urban air quality management policies in the 21st century relies upon an accurate understanding of the relative contributions from all sources, which are expected to evolve at city, state, and national levels with policies targeting air pollutant and greenhouse gas emissions reductions as well as vehicle electrification.[12] Shifts in human activity with the onset and evolution of the coronavirus disease 2019 (COVID-19) pandemic have brought opportunities to evaluate perturbations in emissions of primary pollutants and precursors to secondary pollution, which have been explored for a subset of criteria pollutants (e.g., $NO_x$, CO, $PM_{2.5}$) worldwide using available data.[13,14] However, studies directly examining changes in U.S. urban VOC concentrations during the pandemic and their contributions to atmospheric reactivity are limited due to a lack of long-term continuous measurements spanning the shutdown.[15−17]

New York City (NYC), a densely populated metropolitan area of approximately 20 million people, was the first major U.S. city substantially affected by severe acute respiratory syndrome coronavirus 2 (SARS-CoV-2) infections. In response to the pandemic, on March 22, 2020, the *New York State on Pause*[18] order was executed, resulting in dramatic changes in state- and city-level policies, transportation, human behavior,

Received: August 15, 2022
Revised: June 4, 2023
Accepted: June 5, 2023
Published: June 16, 2023

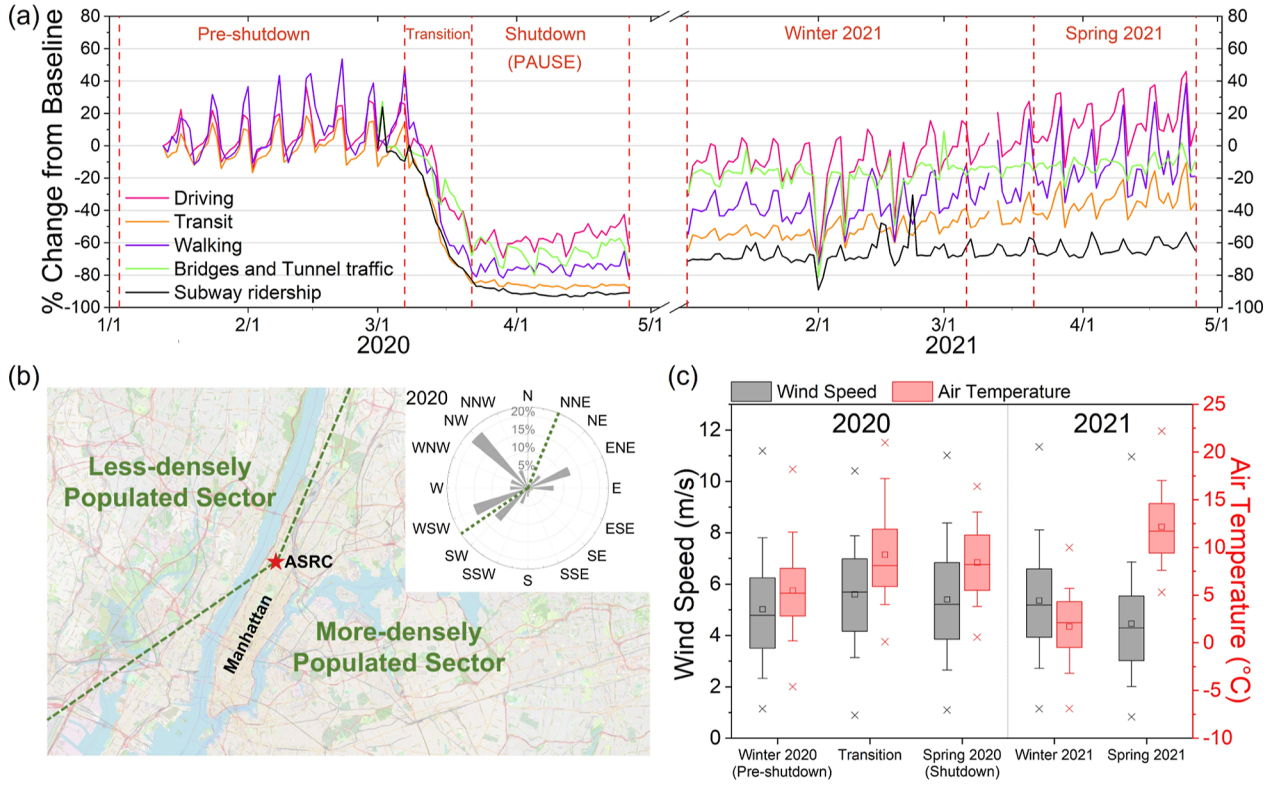


**Figure 1.** (a) Changes in human mobility (driving, walking, and transit) in New York City along with subway ridership and bridge/tunnel traffic shown over the 2020 period preceding and during the shutdown and the corresponding 2021 period, from Apple Mobility[32] and the Metropolitan Transportation Authority.[33] (b) Location of the sampling site in upper Manhattan with a windrose for the 2020 observation period, where the green dash lines demarcate the more densely populated urban sector and the less densely populated sector. Map prepared with an OpenStreetMap layer in qGIS (©OpenStreetMap contributors, https://www.openstreetmap.org/copyright. Adapted with permission from OpenStreetMap, changes were made to the copyrighted material, https://creativecommons.org/licenses/by/3.0/). (c) Wind speed and air temperature in the more densely populated sector during pre-shutdown (January 3−March 6), transition (March 7−March 21), and shutdown (March 22−April 26) periods in 2020, shown with winter (January 3−March 6) and spring (March 22−April 26) 2021 (whiskers: 10th and 90th percentiles; markers: 1st and 99th percentiles).

and economic activity in New York and nearby New Jersey (Figure 1a). The onset and evolution of COVID-19 in America's largest city provided a unique opportunity to evaluate real-world observations that reflect a simulation of future changes in air pollutant emissions associated with lower fossil fuel use. This dynamic was captured with continuous VOC measurements in NYC immediately before, during, and after COVID-19-related changes in anthropogenic activity, allowing for evaluation of the relative importance of various sources for some trace gases under future anthropogenic emission scenarios.

We evaluate two scenarios with this multi-year dataset: (i) the sharp decrease in VOC emissions with changes in urban human activity during the COVID-19 shutdown (in winter and spring 2020), and (ii) increases in VOC emissions with higher temperatures expected under a changing climate using observations during the unseasonably warm spring of 2021. Specifically, (a) we examine changes in the abundance and temporal dynamics of key VOCs that are indicators of various source types using continuous data in Manhattan, NYC, before and during the COVID-19 shutdown, and for the same dates in 2021. (b) We compare these changes in VOCs against human activity and meteorology to examine the role of key source types and ambient temperatures. (c) We then use these results to constrain the relative potential impacts of these changes in VOC emissions on atmospheric reactivity to inform analogous projected future changes in anthropogenic emissions and climate that will impact urban air quality in this century.

## 2. MATERIALS AND METHODS

On January 3, 2020, we began making continuous, high-resolution measurements of a subset of key VOCs as well as carbon monoxide (CO) from the rooftop observatory at the Advanced Sciences Research Center (ASRC) of the City University of New York (40°48′56″N, 73°57′1″W at 85 St Nicholas Terrace). Continuous measurements extended through the COVID-19-related shutdown (March 22−April 26, 2020) and again during the subsequent winter and spring (January 3−March 6 and March 22−April 26, 2021). Air was continuously sampled from the rooftop observatory that is situated ∼90 meters above sea level on one of the tallest buildings in the vicinity of the site, where the inlet is located on the SE corner of the building rooftop at ∼2 meters above roof level. Coincident measurements of wind speed and direction were used to partition two incoming wind sectors reflective of population density with a more densely populated upwind area (that included Manhattan, the Bronx, Queens, Brooklyn, and parts of metro NYC in New Jersey) and a less densely populated region that included the relatively less densely populated northerly sector (Figure 1).

The analysis is broken down into distinct time periods defined by the phase of the 2020 shutdown and the analogous



https://doi.org/10.1021/acs.est.2c05904
Environ. Sci. Technol. 2023, 57, 9683−9692

seasons in 2021 with a return to more typical human activity levels (city-wide data; from Apple Mobility and the Metropolitan Transportation Authority) (Figure 1a). In 2020, vehicle and pedestrian traffic remained relatively constant from January 3 to March 7 during the "pre-shutdown" period, but from March 7 to 21, travel and activity reduced sharply during the "transition" period with varied individualized changes in human activity. Starting March 22, all nonessential businesses were closed in the state of New York, and traffic and human activity remained low with dramatic mobility reductions through the end of April 2020, then gradually increased into 2021 (Figure 1a).

**2.1. Volatile Organic Compounds.** VOCs were measured using online high-resolution proton-transfer time-of-flight mass spectrometry (HR-PTR-ToF-MS; Ionicon 8000, Analytik GmbH, Austria). The basic principle of PTR-ToF-MS has been described previously,[19,20] with additional details on instrument specifics and data processing methodology in the Supporting Information and cited literature.[21] This instrument has excellent temporal resolution and is suitable for long-term continuous measurements, with the limitations that identification of the compounds is based on ion mass, so isomers cannot be distinguished, and analyte ionization via $H_3O^+$ is susceptible to fragmentation. Standard gas calibrations were performed using a dynamic dilution system. VOC-free air was produced by pumping ambient air through a Pt-based catalytic converter at 400 °C. We used two different gravimetrically prepared standard gases (Apel-Reimer Environmental Inc.), with seven primary compounds [acetaldehyde, acetone, isoprene, methacrolein, methyl ethyl ketone (MEK), toluene, alpha-pinene, and decamethylcyclopentasiloxane ($D_5$)] each at ∼1 ppm concentration. The calibration gas was dynamically diluted by the VOC-free air and analyzed using the PTR-ToF-MS. Calibration was performed spanning a concentration range of observed values (0, 5, 10, 15, and 20 ppb). The calibration gas was typically analyzed twice a week prior to the shutdown and typically every 1−2 weeks during the shutdown, given limited access to the observatory during the shutdown in NYC. More details are provided in the Supporting Information for calculated calibrations for species without standards.

For this analysis, we quantified 16 separate ions, with each $m/z$ signal representing one or more specific compounds. These 16 ions include some of the most abundant species present in the data, are a reflection of one or more source types, and represent a major fraction of gas phase VOCs in terms of their mass or reactivity. For example, benzene and toluene, along with CO (measured by CRDS, see below), are excellent tracers of combustion processes (including motor vehicles), while $D_5$ is a species specifically reflective of personal care products. Species such as isoprene are largely, but not exclusively, emitted from biogenic processes, particularly in the summer. Monoterpenes are emitted from both anthropogenic and biogenic sources, while other measured reactive species may have both primary and secondary sources (e.g., methanol, acetaldehyde, and formaldehyde). All data were integrated at 5 min intervals, grouped by wind direction into the more and less densely populated sectors (Figure 1b) for targeted analysis of the area with the highest population density, where the bulk of emissions occur in proximity to the site, and the influence of chemical losses for the target VOCs within this footprint (discussed below, Figure S1) is minimized during winter to early spring months but likely plays a greater role in future summertime studies at the site.

**2.2. Carbon Monoxide and Meteorology.** Measurements of CO were made using a Picarro G2401-m (2020) and a Picarro G2401 (2021) and calibrated to the NOAA X2014 A calibration scale. Both analyzers reported data every 2−3 s and averaged to 5 min data to match the rudimentary meteorological data (wind speed, wind direction, air temperature, relative humidity) that was recorded at 5 min averages measured by an ATMOS 41 Weather Station, which was colocated with the VOC sampling inlet. Given the dynamic changes in wind direction at the site, the classification into more vs less densely populated sectors, diurnal profiles, and period-wide average concentrations were determined from 5 min resolution data (matching the weather station) to effectively isolate data by wind direction and minimize variance due to changing wind direction. The more densely populated sector was defined by wind directions spanning from NNE (23°) to SW (235°), and the less densely populated sector included wind directions from SW (236°) to NNE (22°). We also filtered data (∼4%) with elevated benzene/toluene ratios exceeding 1.0 ppb $ppb^{-1}$ and benzene concentrations over 0.5 ppb to conservatively remove the influence of biomass burning from our analyses,[22,23] which were principally observed to the west in the relatively less densely populated sector (Figures S2 and S3).

**2.3. Hydroxyl Radical Reactivity.** The absolute value of hydroxyl radical (OH) reactivity (known as the OH loss rate) has been used to estimate the total amount of reactive species in an air mass or the $RO_2$ production rate. It is equivalent to the inverse of the lifetime of OH radicals ($s^{-1}$) in the presence of those atmospheric constituents and is used as a parameter for analyzing the total amount of reactive species in the atmosphere.[24,25] Whereas tropospheric OH concentration is variable and determined by photolytic and recycling sources from the $HO_x$-$RO_x$ radical pool.[26] The chemical speciation of the reactive VOCs also carries air quality-relevant implications, such as SOA yield, which is directly tied to molecular properties such as volatility, hygroscopicity, viscosity, and condensed-phase reactivity.[27] In this study, we define OH* reactivity (OHR*) as the sum of the products of the concentrations of the measured VOCs (Table S1) and CO multiplied by their respective rate constants with OH radical (eq 1). OHR* is then calculated for the different time periods (pre-shutdown, transition, shutdown, winter 2021, spring 2021) and compared between periods (2).

$$\mathrm{OHR}^{*} = \sum_{i}^{n} k_{\mathrm{OH+X}_i}\,[\mathrm{X}_i] \tag{1}$$

$$\Delta\mathrm{OHR}^{*}_{\mathrm{decrease}} = [\mathrm{OHR}^{*}_{\mathrm{shutdown}} - \mathrm{OHR}^{*}_{\mathrm{pre\text{-}shutdown}}] / \mathrm{OHR}^{*}_{\mathrm{pre\text{-}shutdown}} \tag{2}$$

$$\Delta\mathrm{OHR}^{*}_{\mathrm{increase}} = [\mathrm{OHR}^{*}_{\mathrm{spring\ 2021}} - \mathrm{OHR}^{*}_{\mathrm{pre\text{-}shutdown}}] / \mathrm{OHR}^{*}_{\mathrm{pre\text{-}shutdown}} \tag{3}$$

In eq 1, $X_i$ represents the VOCs in Table S1 and CO, and $k_{\mathrm{OH+X}_i}$ represents the rate constant rate for each compound with the OH radical, which is shown in Table S2.

## 3. RESULTS AND DISCUSSION

**3.1. Meteorology Influences during the Study Period.** In order to compare measurements at the site across different



https://doi.org/10.1021/acs.est.2c05904
Environ. Sci. Technol. 2023, 57, 9683−9692

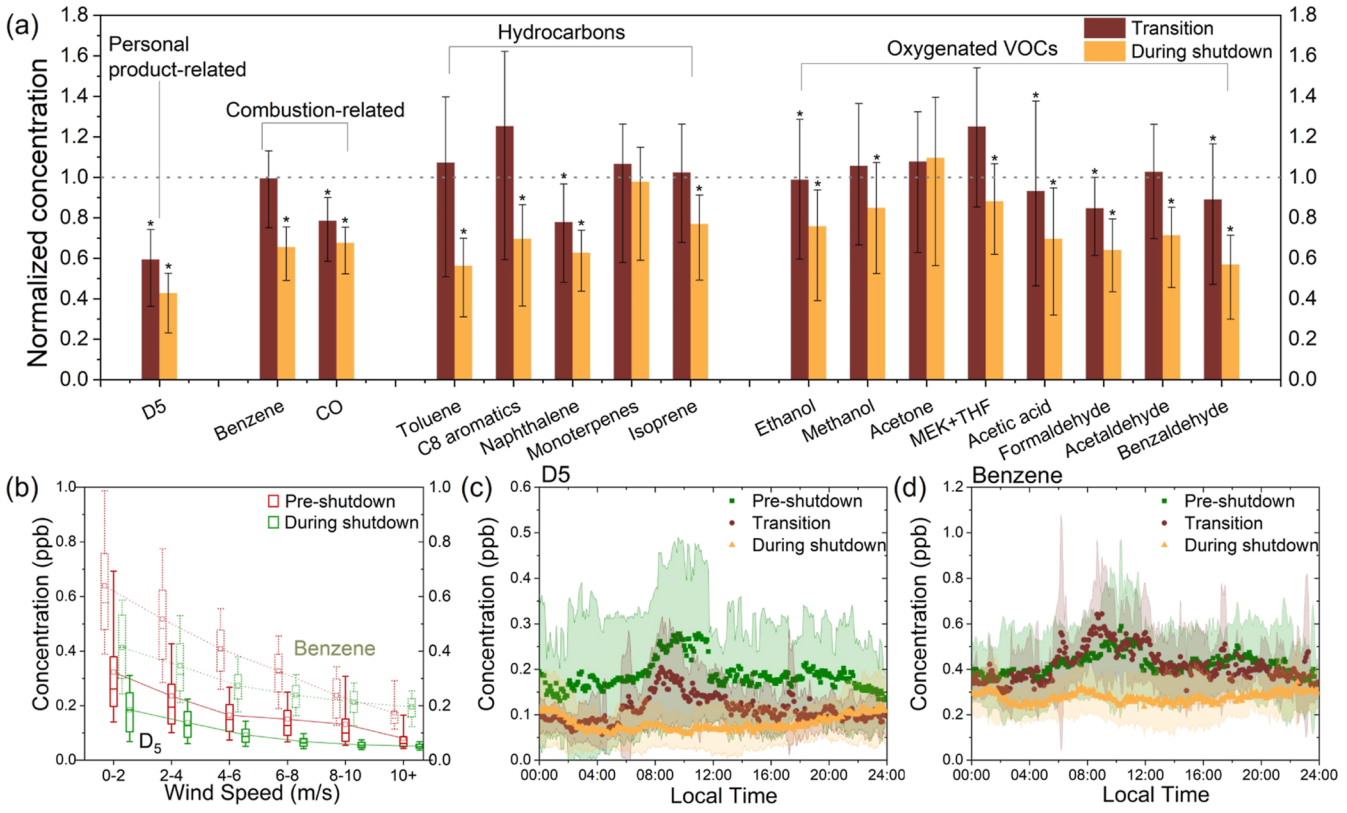


**Figure 2.** Effects of the 2020 shutdown on ambient VOC concentrations. (a) Observed changes in average concentrations within the more densely populated urban area for selected major VOCs (and CO) grouped by generalized type and shown for the transition (brown) and shutdown periods (orange), with averages and interquartile ranges normalized to the pre-shutdown arithmetic mean (note: the geometric means agree well with the arithmetic means, shown in Figure S13). The asterisks in panel 2a indicate if changes in compound concentrations during transition or shutdown periods were significantly lower (one-sided Mann−Whitney Wilcoxon test) than concentrations during the pre-shutdown period (e.g., Figure S14). (b) Average concentrations of benzene (dotted lines) and $D_5$ (solid lines) during the pre-shutdown and shutdown periods in the more densely populated sector as a function of wind speed, shown with the 10th, 25th, 75th, and 90th percentiles and medians (box and whisker plots) and arithmetic averages (squares with connecting lines). (c,d) Diurnal variations in $D_5$ and benzene concentrations in the densely populated sector (shaded areas represent standard deviations). See Figures S10 and S15 for more VOC diurnal profiles and temporal resolution on the $D_5$ changes across the stages of the shutdown.

time periods and between years, we examined variations in key meteorological parameters [e.g., wind speed, wind direction, surface temperature, and planetary boundary layer (PBL) height] between each period and then analyzed the VOC observations across the time periods with attention to similarities or variations in meteorology. For the more densely populated sector, similar wind speed distributions were observed across the three 2020 periods (Figure 1c), with mean wind speeds (25th percentile, 75th percentile) of 5.0 (3.5, 6.2), 5.6 (4.2, 7.0), and 5.4 (3.9, 6.8) m/s during pre-shutdown, transition, and shutdown periods, respectively. For comparison, mean wind speeds (and percentiles) from the less densely populated sector were slightly higher, at 5.8 (3.5, 7.4), 5.7 (3.9, 7.2), and 5.9 (3.6, 7.3) m/s in each period, respectively (Figure S4). Within the densely populated wind sector, we observed strong inverse relationships between VOC concentrations and wind speed (e.g., Figure 2b). By comparison, regional PBL height had less influence on VOC concentrations (Figure S5), and wind speeds and PBL heights were not well correlated (Figures S6 and S7). Thus, wind speed was a better indicator of dilution of local VOC emissions within the short transport distances to the site given its role in both advection and turbulent mixing of surface-level emissions.

To examine the areas of the more densely populated sector that influenced the observations at the site, we generated and analyzed footprints from HRRR-STILT for each time period (see Supporting Information Section S2.7), which combines NOAA High-Resolution Rapid Refresh (HRRR) meteorological data with the Stochastic Time-Inverted Lagrangian Transport (STILT) model. HRRR-STILT calculates the relative surface influence, which describes where and for how long air spent interacting with the surface before being sampled. The HRRR meteorology accounts for the previously mentioned metrics related to transport, including temperature, PBL height, wind speed, and wind direction, and we use this quantity here to examine the distribution of areas around the site that influence the observed VOC concentrations and variations across study time periods. The footprint results (Figure S1) are consistent with our choice of wind sectors. The extent and intensity of surface influence in each sector varies minimally between winter 2020, spring 2020, and winter 2021. Spring 2021 shows slightly more influence from the south, consistent with southerly winds and warmer temperatures.

Temperature can also be an important driver of VOC emissions and thus air quality, with traditional examples being biogenic emissions and evaporative emissions from anthropogenic sources and temperature-dependent ambient observations including VOCs and oxidation products.[28−31] It is expected that intra- and inter-annual variations in temperatures may influence variations in VOC emissions (and perhaps


https://doi.org/10.1021/acs.est.2c05904
Environ. Sci. Technol. 2023, 57, 9683−9692

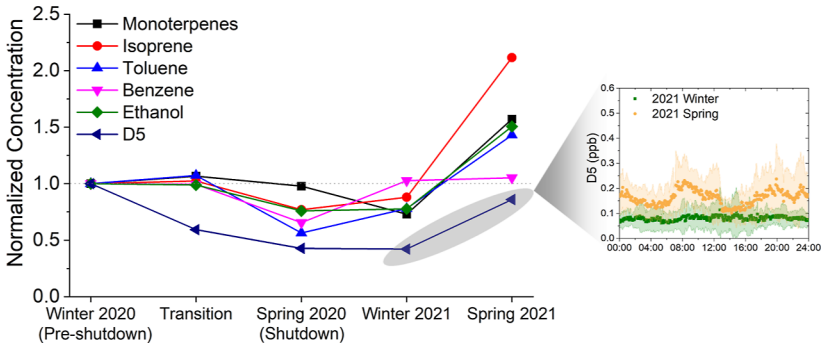


**Figure 3.** Relative changes in select VOC abundances in the more densely populated sector across the 2020−2021 study periods, including increasing human activity levels in 2021. The changes across 2020 and 2021 observations are each normalized to pre-shutdown concentrations, and the inset (right) shows $D_5$ diurnal patterns in 2021 (for the more densely populated sector), including a return of the morning commute spike (see Figures S16 and S17 for all compounds and a similar summary of human activity levels, and Table S1 for standard deviations across each period).

secondary production of oxygenated VOCs); thus, we compare average temperatures across the 2020 shutdown and during the same time periods in 2021. For the densely populated sector, temperature increases across the 2020 study period were small (Figure 1c), increasing from an average of 5.5−8.4 °C between winter (pre-shutdown) and early spring (shutdown), which is mostly a reflection of the relatively warm winter (Figure S8a,b). In contrast to this, the average temperature increases across the same period in 2021 were significantly larger (i.e.,1.7−12.1 °C, respectively), which is mostly a reflection of an unusually warm spring 2021 (Figure S8c,d), with temperatures of 12.1 ± 3.8 °C in the more densely populated sector and observed daytime highs averaging 17.3 ± 3.7 °C (range: 11.2−26 °C).

**3.2. Dynamic Changes in VOC Concentrations and Temporal Patterns Observed during the 2020 Shutdown.** The dramatic shifts in human behavior during the 2020 economic shutdown had considerable impacts on ambient VOC concentrations and their diurnal patterns, with statistically significant decreases in most VOCs despite similar wind speed distributions (Figure 2a). The 57 and 66% decreases in driving activity and bridge/tunnel traffic (a proxy for reduced traffic across the city), respectively (Figure 1a), were accompanied by observed reductions in the combustion-derived pollutants benzene (−34%) and CO (−32%) during the shutdown.

Reductions in some VOCs occurred more immediately with the sharper decreases in walking, transit use, and subway ridership during the onset of the pandemic compared to driving activity, which did not decrease as abruptly (Figures 1a and S9). We observed an immediate 40% reduction in the concentration of $D_5$, a VOC related to personal care products (e.g., deodorants), during the transition period. This was followed by a 57% reduction during the shutdown that saw dramatic reductions in walking (−75%), subway ridership (−91%), and overall transit use (−86%). By comparison, combustion/vehicular-related VOCs (e.g., benzene) lagged with a more marked drop during the shutdown (Figures 2a,d and S10), consistent with human activity data (Figure 1a). Other VOCs, which are emitted from a mix of sources, generally decreased in the more densely populated sector during the shutdown at statistically significant levels ranging from 10 to 44% (Figure 2a). Notably, average monoterpene concentrations remained similar (Figure S10), and acetone concentrations even increased slightly on average, though may have been influenced by temperature-dependent source(s) (discussed below).

The overall shifts in human behavior (Figure 1a) dramatically influenced the temporal patterns of VOC emissions from diurnally variable human activities that are often important sources of reactive pollutants (e.g., VOCs) and drivers of atmospheric concentrations.[34,35] Independent from decreases in absolute concentrations, the shutdown brought evident reductions in peak daytime concentrations that are often associated with periods of commuting (via vehicle, transit, or walking), commercial services, or other outdoor human activities. The result was a smoothing out of daytime concentration dynamics in the highly populated (and less dense) sectors for most VOCs (Figure 2c,d) that is further shown by changes in $D_5$ concentrations resolved over the winter and spring months (Figure S10). Like $D_5$ and benzene (Figure 2c,d), many compounds showed a dampening of the diurnal cycle during the shutdown that included a shift from daytime maxima coinciding with human activity to broad maxima at lower concentrations, in many cases at night (with reduced dilution) (Figure S10). For VCPs, the minimized outdoor activity likely increased the relative contribution of indoor-to-outdoor transport[36−38] for VOCs with indoor sources that would be slowly ventilated out of homes at relatively constant rates (e.g., acetone, ethanol, monoterpenes, acetic acid) and in the case of may be less sensitive to temporary population reductions in Manhattan during the shutdown (Figure S11, Section S2.5).

In spite of these dramatic changes, overall VOC/CO ratios in NYC remained largely similar during the shutdown (Figure S12), although there were weak correlations between VOCs and CO (at 5 min resolution), likely due to the diversity of urban sources with varying emissions of VOCs and/or CO. Given the substantial decreases in traffic, outdoor human activities, and VCP-related commercial activities, coincident emissions reductions across the multifaceted mix of urban sources resulted in generally similar VOC/CO ratios for many of the measured compounds. However, there were somewhat elevated ratios for some VOCs that did not decrease (e.g., monoterpenes, acetone) and lower $D_5$/CO ratios due to the substantial decrease in $D_5$ (Figure 2a,c). Additionally, the shutdown similarly brought decreases in most VOCs, albeit smaller, from the relatively less densely populated sector (Tables S1, S3 and Figure S10).

**3.3. Changes in VOC Concentrations during 2021 with Ongoing Shifts in Human Behavior.** 2021 brought a



https://doi.org/10.1021/acs.est.2c05904
Environ. Sci. Technol. 2023, 57, 9683−9692

slow return to typical human activity that was partly inhibited by a wintertime surge in COVID-19 cases (i.e., the alpha variant) and a delayed return to in-person schooling in mid-late March. By spring 2021, a reduction in cases and increased vaccination led to more typical human activity levels and patterns (relative to pre-shutdown 2020), albeit with diminished subway ridership (Figure S16). VOCs that had decreased with the shutdown saw varying rates of recovery across winter and spring 2021 (Figure 3). For example, benzene abundances were similar to pre-shutdown levels by winter 2021, during which average driving activity and bridge/tunnel traffic reached 84 and 77% of pre-shutdown levels, respectively. Whereas, overall $D_5$ concentrations remained low in winter 2021 with limited diurnal variations until spring 2021, at which time concentrations increased to near pre-shutdown levels and clear diurnal dynamics re-emerged with morning commute and afternoon/evening maxima (Figure 3 inset). Concentrations of most other VOCs also remained below pre-shutdown levels during winter 2021 in the more densely populated sector before increased average concentrations were observed in spring 2021 (Figure 3 and S17) and a return of diurnal dynamics that were more similar to pre-shutdown patterns (Figure S10). However, while benzene and $D_5$ returned to around pre-shutdown average concentrations in spring 2021 (along with methanol and naphthalene), most other VOCs had average concentrations that were 40−120% above pre-shutdown levels.

These substantial spring 2021 increases in VOC concentrations in the more densely populated sector coincided with large increases in ambient temperature relative to spring 2020 and other periods (Figure 1c and Table S1), as well as increases in outdoor human activity (e.g., walking) without the shutdown (Figure 1a). A comparison to the observed enhancement in the less densely populated sector, which included prominent northwesterly flows (i.e., ∼30% total from WNW−NW, Figure S18), provides valuable comparisons to regional concentrations and their relative changes over the same time periods. For the less densely populated sector, spring 2021 changes (relative to winter 2021) were limited to ±25% for all observed VOCs with the exception of acetaldehyde (+29%), monoterpenes (+57%), and isoprene (+86%) (Figure S19). By comparison, the densely populated sector had increases of 60−140% for most VOCs, which were also reflected in the re-emergence of daytime diurnal profiles indicative of anthropogenic emission patterns (Figure S10). It is also notable that the increased temperatures coincided with larger absolute concentrations in the more densely populated sector compared to the less densely populated sector. With the exception of formaldehyde, average VOC concentrations were greater by 40−200% in the more densely populated sector in spring 2021 (Table S1), with more variable diurnal profiles for most compounds (Figure S10). Whereas, the relative enhancements between sectors were smaller (13−56% across all compounds) during the colder winter 2020 period prior to the shutdown (Table S1).

**3.4. Relative Contributions of Motor Vehicle VOC Emissions and Other Sources Influencing NYC Air Quality.** NYC and other urban areas have diverse mixes of VOC sources with uncertain relative contributions that are changing over time with air pollution policy and climate. Here, we discuss the observations across the 2020 shutdown, the subsequent recovery, and the warmer spring 2021 in the context of the underlying sources contributing to reactive VOCs that influence air quality in urban areas and downwind.

The changes in VOC abundances (and their diurnal patterns) during the shutdown and subsequent recovery provide valuable constraints on the impact that dramatic reductions in motor vehicle traffic had on related VOC emissions. Some VOCs were strongly influenced by these changes, while others had more limited decreases attributable to mobile sources. For example, the reductions in benzene concentrations in the more densely populated sector were well correlated with average changes in driving activity across the 2020−2021 periods ($r$ = 0.97, Figure S20). However, there are other, non-vehicle-related, sources contributing benzene (and co-emitted VOCs) to NYC. First, there is evidence for this in the 0.17 ppb intercept of the benzene vs. driving regression, while similar latitude background measurements were 0.07 ± 0.02 ppb (Niwot Ridge, CO)[39] and the fifth percentile of all NYC benzene data was 0.13 ppb (this study). This 0.17 ppb intercept suggests a lower bound for additional urban benzene sources beyond motor vehicles (and other sources influenced by the shutdown), with possible contributions from building heating (fuel oil is a common fuel used across NYC) and other distributed "area" or "mobile" sources that use fossil fuels. Second, during winter 2020 and 2021 (e.g., January−February), VOC concentrations were periodically influenced by biomass burning source(s) originating from the West (incl. New Jersey), which resulted in benzene concentration spikes reaching up to 10 ppb at the site with benzene/toluene and benzene/CO ratios indicative of biomass burning (Figure S2). While this data was excluded from the analysis of shutdown effects in the less densely populated sector, it highlights local/regional biomass burning source(s) influencing wintertime NYC air quality via VOCs (or $PM_{2.5}$[40]), in addition to the long-distance transport of biomass burning emissions previously observed during summer.[41]

Not all combustion-related VOCs (e.g., aromatics and aldehydes) behaved similarly to benzene, which was more sensitive to the large decrease in driving activity that accompanied the shutdown, similar to that of $NO_x$ in NYC and other urban areas.[14,42] Other VOCs that are partly associated with motor vehicle emissions exhibited relatively less sensitivity to the dramatic reductions in traffic during the shutdown (Figure 2a) or were more influenced by decreased emissions from other sources. To constrain the effect of reductions in mobile source emissions during the shutdown, observed decreases in combustion-related VOCs were compared to expected decreases estimated from observed benzene (or $NO_x$) reductions and each VOC's emission ratio to benzene or $NO_x$ in gasoline or diesel vehicle emissions, respectively (Figure S21).[43,44]

Decreases in $C_8$ aromatic concentrations during the shutdown were only slightly more than expected reductions relative to benzene, while toluene decreases were ∼60% greater than expected (Figure S21a), inferring reductions from other sources, which can be expected given known contributions from other sources (e.g., VCPs) based on both bottom-up and top-down studies.[6,8] Similarly, the observed reductions in oxygenated VOCs that are known products of incomplete combustion (e.g., formaldehyde, acetaldehyde, benzaldehyde, and acetic acid) and photochemical oxidation can only be partially attributed to a drop in gasoline or diesel vehicle emissions (Figure S21b). Whereas, the large decreases in ambient methanol concentrations could not be attributed to


https://doi.org/10.1021/acs.est.2c05904
Environ. Sci. Technol. 2023, 57, 9683−9692

mobile source reductions. Mobile sources only accounted for ~14% of observed ethanol in prior NYC measurements,[8] and during the shutdown we saw some expected reductions with decreases in gasoline-powered vehicular traffic. However, there were apparent increases in ethanol emissions from other sources, offsetting some of these reductions, including those contributing to elevated nighttime concentrations (Figures S10, S14, S22). In all, the observed 2020 reductions were indicative of the extent of VOC reductions expected from policies targeted at motor vehicles and other mobile sources, while also including shutdown-related reductions attributable to other human-related sources, such as VCPs and commercial cooking operations.

**3.5. Role of Temperature-Dependent Urban VOC Emissions.** The concentration increases observed in spring 2021 for many VOCs (Figures 3 and S23) can be partly attributed to increases in outdoor human activity. Yet, the warmer spring weather brought additional increases due to temperature-dependent emissions from a mix of biogenic and anthropogenically influenced sources that were more abundant in the highly populated areas versus the less densely populated sector (Figure S19). Here we discuss the observed temperature-dependent variations for different VOC classes in the more densely populated sector.

*3.5.1. Anthropogenic VOCs.* Benzene increased minimally (e.g., 2−5%) in spring 2021 relative to winter 2020 and winter 2021 (Figure 3), suggesting relatively minor increases in combustion-related emissions (e.g., motor vehicles). In contrast, other anthropogenic VOCs increased substantially compared to both winter 2021 and pre-shutdown winter 2020 levels (Figure S24). Such VOCs include ethanol, toluene, and $C_8$ aromatics, which were 250, 920, and 1070% greater than expected for gasoline-related mobile sources based on the small 0.02 ppb increase observed in benzene between pre-shutdown 2020 and spring 2021. This suggests that these increases in anthropogenic emissions (with potential biogenic contributions in the case of some VOCs) are not combustion-related, instead having greater influence from temperature-dependent evaporative/off-gassing emission pathways. This temperature dependence is further supported by observed increases in VOC/benzene ratios with temperature in higher time resolution data (i.e., 5 min; Figure S25). Similarly, increasing concentrations have been reported for some VOCs across a higher temperature range (e.g., 20−40 °C) in the Los Angeles area[29] and for some anthropogenic sources.[45]

The VOC concentration increases highlight temperature-dependent urban sources within the densely populated area that could be associated with the evaporation of VCPs or other understudied sources, which warrants further research across a broader range of VOCs. Some compounds (e.g., acetone, isoprene) had clear increases across both sectors coinciding with temperature (see Supporting Information; Figures S10, S23, S25, S26), with enhancements that were much more pronounced across the densely populated sector. Monoterpenes had minor spring 2021 enhancements in the less-dense sector (Figure S10). Yet, they exhibited dramatic increases in the high population density sector in spring 2021, with diurnal profiles showing morning and evening maxima suggestive of human activities with similarities to $D_5$ and ethanol diurnal patterns (Figure S10), likely due in part to their use in personal products.[10]

*3.5.2. Biogenic VOCs.* The biogenic VOCs studied here include isoprene, monoterpenes, and oxygenated VOCs, though many may have anthropogenically influenced emissions (e.g., VCPs) or are also secondary products of organic oxidation chemistry. Most exhibited enhancements in the warmer spring 2021 and some temperature dependence (Figures S10, S23 and S25). Among them, isoprene is an interesting case, as it is an abundant and reactive VOC whose emissions are often tied to vegetation in many regions of the world. In the urban environment, sources of isoprene are uncertain,[46] and our results show both a decrease during the shutdown and a larger-than-expected spring 2021 enhancement. The increase was greater than would be expected for biogenic emissions at the relatively low daytime high temperatures of 17.3 ± 3.7 °C because numerous field and lab studies have shown that isoprene emissions from isoprene-producing tree species (e.g., oak, sweetgum) are strongly temperature-dependent (following leaf-out).[46,47]

In 2020, despite generally similar average temperatures (Figure 1c), isoprene (with potential contributions from fragmentation byproducts of other compounds appearing on $[C_5H_8H^+]$)[48−50] showed a statistically significant concentration decrease during the shutdown with a weakening of its diurnal cycle that had a pre-shutdown spike around 10−11 AM that was coincident with $D_5$. In spring 2021, isoprene enhancements were larger in the more densely populated sector (Figure S23), and this divergence grew from January to April 2021 with more dynamic diurnal patterns resulting in average spring concentrations that were double that of the less densely populated sector (0.57 ± 0.20 vs 0.29 ± 0.14 ppb). Together, these results point to additional, understudied urban sources of isoprene (or other $C_5H_8H^+$ ions), consistent with other summertime studies that could not fully explain urban isoprene fluxes,[51] and while isoprene is emitted by humans,[52] it is not a common component of VCP formulations.

Overall, the spring 2021 VOC increases that coincided with warming temperatures may have biogenic contributions, but the larger enhancements in the more densely populated sector indicate that regional increases from biogenic sources alone are not driving the increase during these time periods. Instead, these VOC increases highlight the role of temperature-dependent anthropogenic sources and emissions pathways (e.g., evaporative emissions, indoor-to-outdoor transport via ventilation) or anthropogenically influenced biological or biogenic sources in the more densely populated sector. These results identify key areas of further research across source types with additional instrumentation covering a broader range of atmospheric pollutants and tracking year-over-year changes, as well as their representation in regionally resolved anthropogenic (and biogenic) emissions inventories. Similar to the increasingly common warm weather in spring 2021, under future climate scenarios, biogenic and anthropogenic temperature-dependent emissions are expected to increase and so will their contributions to atmospheric chemistry.

**3.6. Implications for OH Reactivity and Lessons for Future Urban Air Quality under Similar Scenarios.** Activity changes during the COVID-19 shutdown resulted in large decreases in transportation fuel use in the densely populated NYC study area. We use OH reactivity to investigate the change in chemical reactivity that accompanied changes in VOC speciation and abundances over this study. OH reactivity is a widely used metric in the field of air quality to evaluate the impact of changes in atmospheric composition on atmospheric reactivity and possible differences in ozone


https://doi.org/10.1021/acs.est.2c05904
Environ. Sci. Technol. 2023, 57, 9683−9692

formation.[24,53,54] Here, we define OH* reactivity (OHR*) to denote only the inclusion of the species studied here (listed in Figure 2 and Tables S1, S2), where OHR* is the sum of the products of the observed VOC concentrations and respective reaction rate coefficients with OH radicals, the primary atmospheric oxidant. Thus, an increase (or decrease) in OHR* reflects an increase (or decrease) in the overall rate of reaction with the OH radical by the measured atmospheric constituents.

The 2020 shutdown (Figure S27) had a short-term effect on OHR* that recovered and was exceeded by spring 2021 (Figure 4). The reductions in VOC and CO concentrations

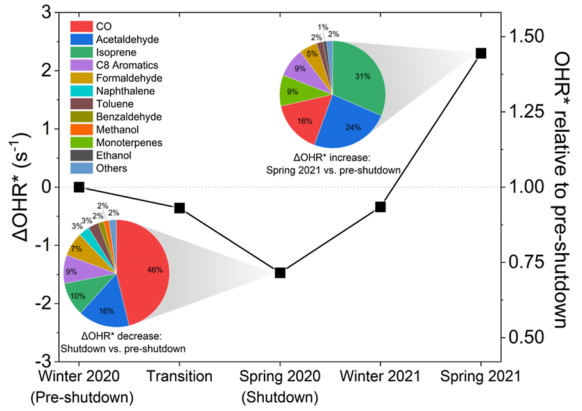


**Figure 4.** Calculated changes in OH reactivity for the subset of species measured in this study (ΔOHR*, left axis), shown normalized to pre-shutdown levels (right axis). The breakdown of compound-specific contributions to ΔOHR* during the 2020 shutdown and spring 2021 compared to the pre-shutdown period is provided in the inset pie charts. See Tables S1 and S3 for standard deviations of VOCs and CO across each period.

during the shutdown resulted in a 28% decrease in OHR*, driven by changes in CO (46%), acetaldehyde (16%), isoprene (10%), $C_8$ aromatics (8%), and formaldehyde (7%). However, during spring 2021, OHR* increased by over 40% compared to both initial pre-shutdown 2020 and exceeding winter 2021 levels. This increase in OHR* was driven by significant temperature-dependent increases in VOC emissions from an uncertain mix of sources and exceeded the potential transportation-related policy gains simulated by the 2020 shutdown. Consequently, rising temperatures under a changing climate risk offsetting some improvements in urban air quality resulting from a transition away from fossil fuels. 21st-century air quality policies necessitate greater attention to the broader range of temperature-sensitive sources expected to play increasing roles in urban air quality under a warming climate.

## ■ ASSOCIATED CONTENT

### Supporting Information

The Supporting Information is available free of charge at https://pubs.acs.org/doi/10.1021/acs.est.2c05904.

Instrument specifics and data analysis methods for PTR-ToF-MS; additional details on data analysis and interpretation; other supporting figures (Figure S1−S27), and tables (Table S1−S5) (PDF)

## ■ AUTHOR INFORMATION


### Corresponding Authors

**Drew R. Gentner** − *Department of Chemical and Environmental Engineering, Yale University, New Haven, Connecticut 06511, United States*; Email: drew.gentner@yale.edu

**John E. Mak** − *School of Marine and Atmospheric Sciences, Stony Brook University, Stony Brook, New York 11794, United States*; orcid.org/0000-0001-8241-5653; Email: john.mak@stonybrook.edu

### Authors

**Cong Cao** − *School of Marine and Atmospheric Sciences, Stony Brook University, Stony Brook, New York 11794, United States*

**Róisín Commane** − *Department of Earth and Environmental Sciences, Columbia University, New York, New York 10027, United States; Lamont-Doherty Earth Observatory, Columbia University, Palisades, New York 10964, United States*; orcid.org/0000-0003-1373-1550

**Ricardo Toledo-Crow** − *Advanced Science Research Center, City University of New York, New York, New York 10031, United States*

**Luke D. Schiferl** − *Lamont-Doherty Earth Observatory, Columbia University, Palisades, New York 10964, United States*; orcid.org/0000-0002-5047-2490

Complete contact information is available at: https://pubs.acs.org/10.1021/acs.est.2c05904


### Author Contributions

Conceptualization: J.E.M., D.R.G., R.C., methodology: C.C., D.R.G., J.E.M., R.C., L.D.S., investigation: C.C., D.R.G., J.E.M., R.C., R.T-C., L.D.S., visualization: C.C., D.R.G., J.E.M., supervision: J.E.M., D.R.G., R.C., writing—original draft: C.C., D.R.G., J.E.M., writing—review and editing: C.C., D.R.G., J.E.M., R.C., R.T-C., L.D.S.

### Notes

The authors declare no competing financial interest.

All data needed to evaluate the conclusions in the paper are present in the paper and/or the Supporting Information. Additional data related to this paper may be requested from the authors.

## ■ ACKNOWLEDGMENTS

C.C., D.R.G., and J.E.M. thank Northeast States for Coordinated Air Use Management (NESCAUM) for funding this research through a contract with the New York State Energy Research and Development Authority (NYSERDA) (agreement no. 101132) as part of the LISTOS project. Any opinions expressed in this article do not necessarily reflect those of NYSERDA or the State of New York. The authors also thank NOAA for funding the research (J.M., R.C., C.C., L.D.S.: NA20OAR4310306; R.C., L.D.S.: NA21OAR4310235), and D.R.G. thanks NSF for support (CBET-2011362). R.C. acknowledges laboratory start-up support from Columbia University. J.E.M. acknowledges support from the Stony Brook Foundation. The authors are grateful to CUNY for hosting the measurements at their rooftop observatory and to NOAA-CSL researchers for helpful discussions.

## REFERENCES


(1) Goldstein, A. H.; Galbally, I. E. Known and Unexplored Organic Constituents in the Earth's Atmosphere. *Environ. Sci. Technol.* **2007**, *41*, 1514−1521.

(2) Jimenez, J. L.; Canagaratna, M. R.; Donahue, N. M.; Prevot, A. S.; Zhang, Q.; Kroll, J. H.; DeCarlo, P. F.; Allan, J. D.; Coe, H.; Ng, N. L.; Aiken, A. C.; Docherty, K. S.; Ulbrich, I. M.; Grieshop, A. P.; Robinson, A. L.; Duplissy, J.; Smith, J. D.; Wilson, K. R.; Lanz, V. A.; Hueglin, C.; Sun, Y. L.; Tian, J.; Laaksonen, A.; Raatikainen, T.; Rautiainen, J.; Vaattovaara, P.; Ehn, M.; Kulmala, M.; Tomlinson, J. M.; Collins, D. R.; Cubison, M. J.; Dunlea, J.; Huffman, J. A.; Onasch, T. B.; Alfarra, M. R.; Williams, P. I.; Bower, K.; Kondo, Y.; Schneider, J.; Drewnick, F.; Borrmann, S.; Weimer, S.; Demerjian, K.; Salcedo, D.; Cottrell, L.; Griffin, R.; Takami, A.; Miyoshi, T.; Hatakeyama, S.; Shimono, A.; Sun, J. Y.; Zhang, Y. M.; Dzepina, K.; Kimmel, J. R.; Sueper, D.; Jayne, J. T.; Herndon, S. C.; Trimborn, A. M.; Williams, L. R.; Wood, E. C.; Middlebrook, A. M.; Kolb, C. E.; Baltensperger, U.; Worsnop, D. R.; et al. Evolution of organic aerosols in the atmosphere. *Science* **2009**, *326*, 1525−1529.

(3) Qin, M.; Murphy, B. N.; Isaacs, K. K.; McDonald, B. C.; Lu, Q.; McKeen, S. A.; Koval, L.; Robinson, A. L.; Efstathiou, C.; Allen, C.; Pye, H. O. T. Criteria pollutant impacts of volatile chemical products informed by near-field modelling. *Nat. Sustain.* **2020**, *4*, 129−137.

(4) Pye, H. O. T.; Ward-Caviness, C. K.; Murphy, B. N.; Appel, K. W.; Seltzer, K. M. Secondary organic aerosol association with cardiorespiratory disease mortality in the United States. *Nat. Commun.* **2021**, *12*, 7215.

(5) Pye, H. O. T.; Appel, K. W.; Seltzer, K. M.; Ward-Caviness, C. K.; Murphy, B. N. Human-Health Impacts of Controlling Secondary Air Pollution Precursors. *Environ. Sci. Technol. Lett.* **2022**, *9*, 96−101.

(6) McDonald, B. C.; de Gouw, J. A.; Gilman, J. B.; Jathar, S. H.; Akherati, A.; Cappa, C. D.; Jimenez, J. L.; Lee-Taylor, J.; Hayes, P. L.; McKeen, S. A.; Cui, Y. Y.; Kim, S.-W.; Gentner, D. R.; Isaacman-VanWertz, G.; Goldstein, A. H.; Harley, R. A.; Frost, G. J.; Roberts, J. M.; Ryerson, T. B.; Trainer, M. Volatile chemical products emerging as largest petrochemical source of urban organic emissions. *Science* **2018**, *359*, 760−764.

(7) Khare, P.; Gentner, D. R. Considering the future of anthropogenic gas-phase organic compound emissions and the increasing influence of non-combustion sources on urban air quality. *Atmos. Chem. Phys.* **2018**, *18*, 5391−5413.

(8) Gkatzelis, G. I.; Coggon, M. M.; Mcdonald, B. C.; Peischl, J.; Gilman, J. B.; Aikin, K. C.; Robinson, M. A.; Canonaco, F.; Prevot, A. S. H.; Trainer, M.; Warneke, C. Observations Confirm that Volatile Chemical Products Are a Major Source of Petrochemical Emissions in U.S. Cities. *Environ. Sci. Technol.* **2021**, *55*, 4332−4343.

(9) Seltzer, K. M.; Murphy, B. N.; Pennington, E. A.; Allen, C.; Talgo, K.; Pye, H. O. T. Volatile Chemical Product Enhancements to Criteria Pollutants in the United States. *Environ. Sci. Technol.* **2022**, *56*, 6905−6913.

(10) Coggon, M. M.; Gkatzelis, G. I.; Mcdonald, B. C.; Gilman, J. B.; Schwantes, R. H.; Abuhassan, N.; Aikin, K. C.; Arend, M. F.; Berkoff, T. A.; Brown, S. S.; Campos, T. L.; Dickerson, R. R.; Gronoff, G.; Hurley, J. F.; Isaacman-Vanwertz, G.; Koss, A. R.; Li, M.; Mckeen, S. A.; Moshary, F.; Peischl, J.; Pospisilova, V.; Ren, X.; Wilson, A.; Wu, Y.; Trainer, M.; Warneke, C. Volatile chemical product emissions enhance ozone and modulate urban chemistry. *Proc. Natl. Acad. Sci. U.S.A.* **2021**, *118*, No. e2026653118.

(11) Seltzer, K. M.; Pennington, E.; Rao, V.; Murphy, B. N.; Strum, M.; Isaacs, K. K.; Pye, H. O. T. Reactive organic carbon emissions from volatile chemical products. *Atmos. Chem. Phys.* **2021**, *21*, 5079−5100.

(12) The White House. FACT SHEET: President Biden Sets 2030 Greenhouse Gas Pollution Reduction Target Aimed at Creating Good-Paying Union Jobs and Securing U.S. Leadership on Clean Energy Technologies. https://www.whitehouse.gov/briefing-room/statements-releases/2021/04/22/fact-sheet-president-biden-sets-2030-greenhouse-gas-pollution-reduction-target-aimed-at-creating-good-paying-union-jobs-and-securing-u-s-leadership-on-clean-energy-technologies/ (accessed April 08 2022).

(13) Goldberg, D. L.; Anenberg, S. C.; Griffin, D.; Mclinden, C. A.; Lu, Z.; Streets, D. G. Disentangling the Impact of the COVID-19 Lockdowns on Urban $NO_2$ From Natural Variability. *Geophys. Res. Lett.* **2020**, *47*, 1−11.

(14) Tzortziou, M.; Kwong, C. F.; Goldberg, D.; Schiferl, L.; Commane, R.; Abuhassan, N.; Szykman, J. J.; Valin, L. C. Declines and peaks in $NO_2$ pollution during the multiple waves of the COVID-19 pandemic in the New York metropolitan area. *Atmos. Chem. Phys.* **2022**, *22*, 2399−2417.

(15) Gkatzelis, G. I.; Gilman, J. B.; Brown, S. S.; Eskes, H.; Gomes, A. R.; Lange, A. C.; Mcdonald, B. C.; Peischl, J.; Petzold, A.; Thompson, C. R.; Kiendler-Scharr, A. The global impacts of COVID-19 lockdowns on urban air pollution. *Elementa* **2021**, *9*, 1−46.

(16) Van Rooy, P.; Tasnia, A.; Barletta, B.; Buenconsejo, R.; Crounse, J. D.; Kenseth, C. M.; Meinardi, S.; Murphy, S.; Parker, H.; Schulze, B.; Seinfeld, J. H.; Wennberg, P. O.; Blake, D. R.; Barsanti, K. C. Observations of Volatile Organic Compounds in the Los Angeles Basin during COVID-19. *ACS Earth Space Chem.* **2021**, *5*, 3045−3055.

(17) Jensen, A.; Liu, Z.; Tan, W.; Dix, B.; Chen, T.; Koss, A.; Zhu, L.; Li, L.; Gouw, J. Measurements of Volatile Organic Compounds During the COVID-19 Lockdown in Changzhou, China. *Geophys. Res. Lett.* **2021**, *48*, 1−11.

(18) New York State Governor. Governor Cuomo Signs the 'New York State on PAUSE' Executive Order. https://www.governor.ny.gov/news/governor-cuomo-signs-new-york-state-pause-executive-order (accessed April 08 2022).

(19) Yuan, B.; Koss, A. R.; Warneke, C.; Coggon, M.; Sekimoto, K.; de Gouw, J. A. Proton-Transfer-Reaction Mass Spectrometry: Applications in Atmospheric Sciences. *Chem. Rev.* **2017**, *117*, 13187−13229.

(20) de Gouw, J.; Warneke, C. Measurements of volatile organic compounds in the earth's atmosphere using proton-transfer-reaction mass spectrometry. *Mass Spectrom. Rev.* **2007**, *26*, 223−257.

(21) Su, L.; Patton, E. G.; Vilà-Guerau de Arellano, J.; Guenther, A. B.; Kaser, L.; Yuan, B.; Xiong, F.; Shepson, P. B.; Zhang, L.; Miller, D. O.; Brune, W. H.; Baumann, K.; Edgerton, E.; Weinheimer, A.; Misztal, P. K.; Park, J.-H.; Goldstein, A. H.; Skog, K. M.; Keutsch, F. N.; Mak, J. E. Understanding isoprene photooxidation using observations and modeling over a subtropical forest in the southeastern US. *Atmos. Chem. Phys.* **2016**, *16*, 7725−7741.

(22) Zhang, Z.; Zhang, Y.; Wang, X.; Lü, S.; Huang, Z.; Huang, X.; Yang, W.; Wang, Y.; Zhang, Q. Spatiotemporal patterns and source implications of aromatic hydrocarbons at six rural sites across China's developed coastal regions. *J. Geophys. Res.: Atmos.* **2016**, *121*, 6669−6687.

(23) Koss, A. R.; Sekimoto, K.; Gilman, J. B.; Selimovic, V.; Coggon, M. M.; Zarzana, K. J.; Yuan, B.; Lerner, B. M.; Brown, S. S.; Jimenez, J. L.; Krechmer, J.; Roberts, J. M.; Warneke, C.; Yokelson, R. J.; de Gouw, J. Non-methane organic gas emissions from biomass burning: identification, quantification, and emission factors from PTR-ToF during the FIREX 2016 laboratory experiment. *Atmos. Chem. Phys.* **2018**, *18*, 3299−3319.

(24) Kim, S.; Guenther, A.; Karl, T.; Greenberg, J. Contributions of primary and secondary biogenic VOC tototal OH reactivity during the CABINEX (Community Atmosphere-Biosphere INteractions Experiments)-09 field campaign. *Atmos. Chem. Phys.* **2011**, *11*, 8613−8623.

(25) Sadanaga, Y.; Yoshino, A.; Kato, S.; Kajii, Y. Measurements of OH Reactivity and Photochemical Ozone Production in the Urban Atmosphere. *Environ. Sci. Technol.* **2005**, *39*, 8847−8852.

(26) Heard, D. E.; Pilling, M. J. Measurement of OH and $HO_2$ in the Troposphere. *Chem. Rev.* **2003**, *103*, 5163−5198.

(27) Kaiser, J.; Skog, K. M.; Baumann, K.; Bertman, S. B.; Brown, S. B.; Brune, W. H.; Crounse, J. D.; de Gouw, J. A.; Edgerton, E. S.; Feiner, P. A.; Goldstein, A. H.; Koss, A.; Misztal, P. K.; Nguyen, T. B.; Olson, K. F.; St Clair, J. M.; Teng, A. P.; Toma, S.; Wennberg, P. O.;




https://doi.org/10.1021/acs.est.2c05904
Environ. Sci. Technol. 2023, 57, 9683−9692

Wild, R. J.; Zhang, L.; Keutsch, F. N. Speciation of OH reactivity above the canopy of an isoprene-dominated forest. *Atmos. Chem. Phys.* **2016**, *16*, 9349−9359.
(28) Nussbaumer, C. M.; Cohen, R. C. The Role of Temperature and $NO_x$ in Ozone Trends in the Los Angeles Basin. *Environ. Sci. Technol.* **2020**, *54*, 15652−15659.
(29) Nussbaumer, C. M.; Cohen, R. C. Impact of OA on the Temperature Dependence of $PM_{2.5}$ in the Los Angeles Basin. *Environ. Sci. Technol.* **2021**, *55*, 3549−3558.
(30) Pusede, S. E.; Gentner, D. R.; Wooldridge, P. J.; Browne, E. C.; Rollins, A. W.; Min, K.-E.; Russell, A. R.; Thomas, J.; Zhang, L.; Brune, W. H.; Henry, S. B.; Digangi, J. P.; Keutsch, F. N.; Harrold, S. A.; Thornton, J. A.; Beaver, M. R.; St Clair, J. M.; Wennberg, P. O.; Sanders, J.; Ren, X.; Vandenboer, T. C.; Markovic, M. Z.; Guha, A.; Weber, R.; Goldstein, A. H.; Cohen, R. C. On the temperature dependence of organic reactivity, nitrogen oxides, ozone production, and the impact of emission controls in San Joaquin Valley, California. *Atmos. Chem. Phys.* **2014**, *14*, 3373−3395.
(31) Pennington, E. A.; Seltzer, K. M.; Murphy, B. N.; Qin, M.; Seinfeld, J. H.; Pye, H. O. T. Modeling secondary organic aerosol formation from volatile chemical products. *Atmos. Chem. Phys.* **2021**, *21*, 18247−18261.
(32) Apple Mobility Trends Reports. https://covid19.apple.com/mobility (accessed April 08, 2022).
(33) MTA Day-by-day ridership numbers. https://new.mta.info/coronavirus/ridership (accessed April 08, 2022).
(34) Coggon, M. M.; McDonald, B. C.; Vlasenko, A.; Veres, P. R.; Bernard, F.; Koss, A. R.; Yuan, B.; Gilman, J. B.; Peischl, J.; Aikin, K. C.; DuRant, J.; Warneke, C.; Li, S. M.; de Gouw, J. A. Diurnal Variability and Emission Pattern of Decamethylcyclopentasiloxane ($D_5$) from the Application of Personal Care Products in Two North American Cities. *Environ. Sci. Technol.* **2018**, *52*, 5610−5618.
(35) Gentner, D. R.; Isaacman, G.; Worton, D. R.; Chan, A. W.; Dallmann, T. R.; Davis, L.; Liu, S.; Day, D. A.; Russell, L. M.; Wilson, K. R.; Weber, R.; Guha, A.; Harley, R. A.; Goldstein, A. H. Elucidating secondary organic aerosol from diesel and gasoline vehicles through detailed characterization of organic carbon emissions. *Proc. Natl. Acad. Sci. U.S.A.* **2012**, *109*, 18318−18323.
(36) Sheu, R.; Stönner, C.; Ditto, J. C.; Klüpfel, T.; Williams, J.; Gentner, D. R. Human transport of thirdhand tobacco smoke: A prominent source of hazardous air pollutants into indoor nonsmoking environments. *Sci. Adv.* **2020**, *6*, No. eaay4109.
(37) Algrim, L. B.; Pagonis, D.; Gouw, J. A.; Jimenez, J. L.; Ziemann, P. J. Measurements and modeling of absorptive partitioning of volatile organic compounds to painted surfaces. *Indoor Air* **2020**, *30*, 745−756.
(38) Arata, C.; Misztal, P. K.; Tian, Y.; Lunderberg, D. M.; Kristensen, K.; Novoselac, A.; Vance, M. E.; Farmer, D. K.; Nazaroff, W. W.; Goldstein, A. H. Volatile organic compound emissions during HOMEChem. *Indoor Air* **2021**, *31*, 2099−2117.
(39) NOAA Global Monitoring Laboratory, *Halocarbons and Trace Gases*, Niwot Ridge, Colorado, United States. https://gml.noaa.gov/dv/iadv/graph.php?code=NWR&program=hats&type=ts (accessed 08 April, 2022).
(40) Chen, Y.; Rich, D. Q.; Hopke, P. K. Long-term $PM_{2.5}$ source analyses in New York City from the perspective of dispersion normalized PMF. *Atmos. Environ.* **2022**, *272*, 118949.
(41) Rogers, H. M.; Ditto, J. C.; Gentner, D. R. Evidence for impacts on surface-level air quality in the northeastern US from long-distance transport of smoke from North American fires during the Long Island Sound Tropospheric Ozone Study (LISTOS) 2018. *Atmos. Chem. Phys.* **2020**, *20*, 671−682.
(42) Bauwens, M.; Compernolle, S.; Stavrakou, T.; Müller, J. F.; Gent, J.; Eskes, H.; Levelt, P. F.; Veefkind, J. P.; Vlietinck, J.; Yu, H.; Zehner, C.; et al. Impact of Coronavirus Outbreak on $NO_2$ Pollution Assessed Using TROPOMI and OMI Observations. *Geophys. Res. Lett.* **2020**, *47*, 1−9.
(43) Gentner, D. R.; Worton, D. R.; Isaacman, G.; Davis, L. C.; Dallmann, T. R.; Wood, E. C.; Herndon, S. C.; Goldstein, A. H.; Harley, R. A. Chemical Composition of Gas-Phase Organic Carbon Emissions from Motor Vehicles and Implications for Ozone Production. *Environ. Sci. Technol.* **2013**, *47*, 11837−11848.
(44) Wu, L.; Chang, M.; Wang, X.; Hang, J.; Zhang, J.; Wu, L.; Shao, M. Development of the Real-time On-road Emission (ROE v1.0) model for street-scale air quality modeling based on dynamic traffic big data. *Geosci. Model Dev.* **2020**, *13*, 23−40.
(45) Khare, P.; Machesky, J.; Soto, R.; He, M.; Presto, A. A.; Gentner, D. R. Asphalt-related emissions are a major missing nontraditional source of secondary organic aerosol precursors. *Sci. Adv.* **2020**, *6*, No. eabb9785.
(46) Kesselmeier, J.; Staudt, M. Biogenic Volatile Organic Compounds (VOC): An Overview on Emission, Physiology and Ecology. *J. Atmos. Chem.* **1999**, *33*, 23−88.
(47) Rasulov, B.; Huve, K.; Bichele, I.; Laisk, A.; Niinemets, U. Temperature response of isoprene emission in vivo reflects a combined effect of substrate limitations and isoprene synthase activity: a kinetic analysis. *Plant Physiol.* **2010**, *154*, 1558−1570.
(48) Gueneron, M.; Erickson, M. H.; VanderSchelden, G. S.; Jobson, B. T. PTR-MS fragmentation patterns of gasoline hydrocarbons. *Int. J. Mass Spectrom.* **2015**, *379*, 97−109.
(49) Warneke, C.; Geiger, F.; Edwards, P. M.; Dube, W.; Pétron, G.; Kofler, J.; Zahn, A.; Brown, S. S.; Graus, M.; Gilman, J. B.; Lerner, B. M.; Peischl, J.; Ryerson, T. B.; De Gouw, J. A.; Roberts, J. M. Volatile organic compound emissions from the oil and natural gas industry in the Uintah Basin, Utah: oil and gas well pad emissions compared to ambient air composition. *Atmos. Chem. Phys.* **2014**, *14*, 10977−10988.
(50) Pagonis, D.; Sekimoto, K.; de Gouw, J. A Library of Proton-Transfer Reactions of $H_3O^+$ Ions Used for Trace Gas Detection. *J. Am. Soc. Mass Spectrom.* **2019**, *30*, 1330−1335.
(51) Kaser, L.; Peron, A.; Graus, M.; Striednig, M.; Wohlfahrt, G.; Juráň, S.; Karl, T. Interannual variability of terpenoid emissions in an alpine city. *Atmos. Chem. Phys.* **2022**, *22*, 5603−5618.
(52) Stönner, C.; Edtbauer, A.; Williams, J. Real-world volatile organic compound emission rates from seated adults and children for use in indoor air studies. *Indoor Air* **2018**, *28*, 164−172.
(53) Kim, S.; Sanchez, D.; Wang, M.; Seco, R.; Jeong, D.; Hughes, S.; Barletta, B.; Blake, D. R.; Jung, J.; Kim, D.; Lee, G.; Lee, M.; Ahn, J.; Lee, S. D.; Cho, G.; Sung, M. Y.; Lee, Y. H.; Kim, D. B.; Kim, Y.; Woo, J. H.; Jo, D.; Park, R.; Park, J. H.; Hong, Y. D.; Hong, J. H. OH reactivity in urban and suburban regions in Seoul, South Korea - an East Asian megacity in a rapid transition. *Faraday Discuss.* **2016**, *189*, 231−251.
(54) Ren, X. HOx concentrations and OH reactivity observations in New York City during PMTACS-NY2001. *Atmos. Environ.* **2003**, *37*, 3627−3637.


https://doi.org/10.1021/acs.est.2c05904
*Environ. Sci. Technol.* 2023, 57, 9683−9692